ings, Phys. Rev. B 4, 2472 (1971).
[12]B. A. Weinstein, Solid State Commun. 24, 595 (1977).
[13]M. T. Yin and M. L. Cohen, J. Phys. Soc. Jpn., Suppl. A 49, 13 (1980).
[14]A. Zunger and A. J. Freeman, Phys. Rev. B 15, 5049 (1977).
[15]V. K. Bashenov and Y. K. Markolenko, Phys. Status Solidi (b) 97, K145 (1980); V. K. Bashenov, Y. K. Markolenko, and V. V. Timofeenko, Fiz. Tverd. Tela 22, 934 (1980) [Sov. Phys. Solid State 22, 549 (1980)].

Fractal (Scaling) Clusters in Thin Gold Films near the Percolation Threshold

R. F. Voss, R. B. Laibowitz, and E. I. Allessandrini
IBM Thomas J. Watson Research Center, Yorktown Heights, New York 10598
(Received 30 June 1982)

Transmission electron micrographs of thin evaporated gold films were analyzed by computer. For length scales above 10 nm, the irregular connected clusters show a perimeter linearly proportional to area. Near the percolation threshold the large-scale power-law correlations and area distributions are consistent with the scaling theory of second-order phase transitions. Geometrically, the boundary of all clusters is a fractal of dimension $D = 2$ while individual boundaries are of fractal dimension $D_C \approx 1.9$.

PACS numbers: 71.30.+h, 05.40.+j, 61.16.Di

A random mixture of conducting (fraction p) and insulating (fraction $1-p$) material abruptly exhibits long-range conduction at a critical concentration $p = p_c$. This simple percolation problem[1] is ideally suited to computer modeling,[1-5] and mathematically equivalent to a second-order phase transition.[6] The rich variety of universal "scaling" behavior near p_c is reflected in the irregular shapes of the connected clusters. Until recently[7] statistical studies of cluster geometry were limited to computer simulations. Conversely, experimental studies of actual materials[8] have been based on conductivity measurements (in spite of the availability of micrographs). In this Letter we present detailed experimental results on the cluster geometry of thin gold films near p_c taken from digitized micrographs. Although local Au-Au and Au-substrate correlations during deposition alter p_c, we find the large-scale properties to be consistent with both scaling theory and computer simulation. Thus, the metal-insulator transition in actual films can belong to the same universality class as the idealized percolation problem.

A mature, analytic scaling theory[1] exists for the percolation transition. Power-law relationships extend over length scales that vary from the model lattice spacing to the correlation length ξ. Near p_c, ξ diverges as $|p-p_c|^{-\nu}$. The characteristic exponents, however, fail to provide an intuitively satisfying description of the intricate, seemingly biological, cluster shapes. Mandelbrot's fractal geometry,[9] on the other hand, offers a natural description in terms of the fractal dimension D of the collected cluster boundaries and the dimension D_C of an individual cluster boundary. Fractals provide an intuitive geometric basis for the scaling behavior, as well as specific geometric models[2,10] for analytic calculations. We shall, therefore, discuss our measurements in terms of both scaling theory and fractals.

The thin Au films were made at room temperature by electron-beam evaporation onto 30-nm-thick amorphous Si_3N_4 windows grown on a Si wafer frame. The deposition rate was 0.5 nm/sec at a base pressure of 2×10^{-7} Torr. Sample thickness was systematically varied with a moving shutter to produce simultaneously a range of samples from 6 to 10 nm thick that varied from electrically insulating to conducting. Transmission electron micrographs were digitized with a scanning microdensitometer (typically on a 512 $\times$ 512 grid). Figure 1(a) shows a halftone representation of one of the digitized images. The structure within each cluster is due to the Au grains. With use of threshold detection and an optimal connectivity-checking algorithm the individual Au clusters were isolated for statistical analysis. In Fig. 1(b) the three largest clusters from Fig. 1(a) are darkest while the remaining clusters are a uniform light gray. At a fractional Au coverage $p = 0.64$, Fig. 1(b) is below p_c and the extent of the largest clusters is less than the

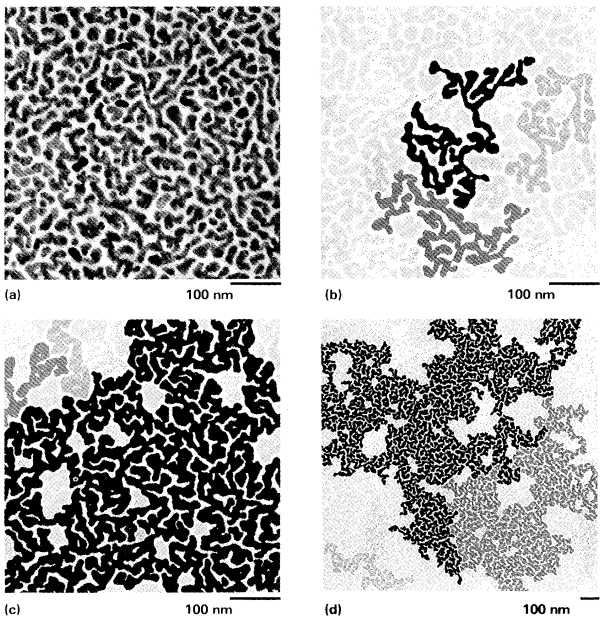

FIG. 1. (a) Halftone representation of a digitized Au cluster transmission electron micrograph. (b) Connectivity analysis of (a) with $p = 0.64$ with the largest clusters shown darkest. (c) Au clusters with $p = 0.75$. (d) Au clusters with $p = 0.71$ at a factor of 3 lower magnification.

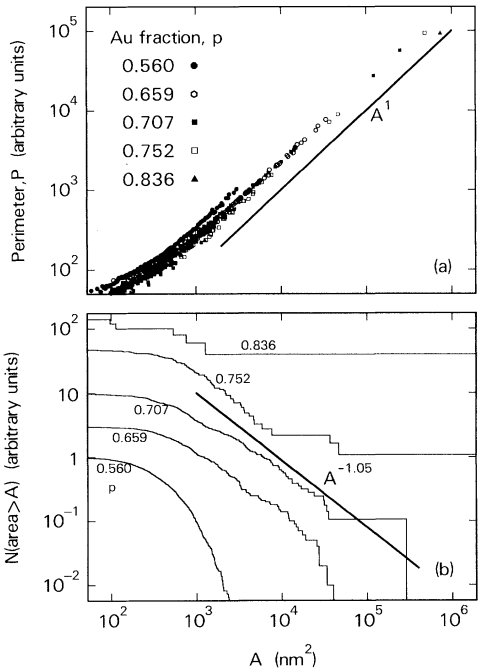

FIG. 2. (a) Perimeter P vs A for the Au clusters at different fractional coverages p. The solid line shows the expected $P \propto A$ at large A. (b) $N(\text{area} > A)$ vs A at the same p. The solid line shows the expected $A^{-1.05}$ dependence at p_c.

field of view. Figure 1(c) with $p = 0.75$ is just above threshold and the largest cluster "connects" all sides. Figure 1(d), at a factor of 3 less magnification, demonstrates the shape of a very large cluster, with $p = 0.71$, just below p_c.

The Au clusters in Fig. 1 are irregularly shaped, "stringy" or "ramified," and certainly not describable as simple Euclidean shapes. Over large scales (>100 nm) the film properties, such as fractional coverage, are uniform. At small scales, however, the Au forms 8–20-nm-wide "sausages" with a 4–8-nm spacing. This metal-insulator asymmetry is presumably due to the initial mobility of the deposited Au atoms combined with surface tension effects. One major consequence is that p_c is about 0.74 ± 0.01, higher than the 0.5 to 0.6 expected from simple two-dimensional lattice models.[2] This effect also sets a lower cutoff (≈ 10 nm) for any scaling properties (similar to a simulation lattice size).

Figure 1 also demonstrates that even when a cluster extends to large distances it remains loosely connected and all points are actually within 10 nm of a boundary. As first suggested by numerical simulation[4] and later proved rigorously,[11] the ramified nature of percolation clusters results in a perimeter P that scales linearly with area A for large clusters. Figure 1(b) also suggests a clustering of the largest Au clusters. The $P \propto A$ dependence is a plausible consequence of large cluster growth by the development of small connecting necks to neighbors. Figure 2(a) shows a scatter plot of P (defined as the number of unoccupied sites on the digitized grid adjacent to a given cluster) as a function of A for some of the films studied at various p. Each point represents one cluster. At large scales ($A > 600$ nm^2) we find the expected $P \propto A$ for all p. A pronounced change from this behavior is, however, seen at small scales. Local correlation gives the smallest clusters ($A < 250$ nm^2) simple, almost circular shapes with $P \propto A^{1/2}$.

Figure 2(a) can also be interpreted geometrically. The topologically one-dimensional cluster boundaries are characterized by a fractal dimension D with $1 < D \leq 2$. D intuitively measures the degree to which the boundaries "fill the plane." The requirement of uniform properties over large areas leads naturally to a dimension d (the Euclidean dimension) = 2 for the clusters them-

selves. The clusters, however, are highly ramified. At large scales they are all boundary and the fractal dimension D of the boundaries (normally $d-1$ for simple Euclidean shapes) becomes the same as that of the clusters, $D=d=2$. In general, Mandelbrot[9] has shown that fractal objects in the plane with boundary dimension D satisfy $P \propto A^{D/2}$. This relation was recently used by Lovejoy[12] to estimate the fractal dimension of cloud and rain area boundaries. Here, the relation immediately yields the observed $P \propto A$ dependence as a consequence of the ramified, "space-filling," nature of the collected cluster boundaries with $D=2$. At small scales the almost circular clusters have a boundary $D=d-1=1$ and $P \propto A^{1/2}$.

The scaling theory of percolation[1] is based on $n_A(p)$, the average number (per lattice site) of clusters of area A as a function of p. At p_c there is no characteristic size scale and $n_A \propto A^{-\tau}$. The exponent satisfies $\tau = 2 + 1/\delta \approx 2.05$ in two dimensions. Similarly, the Korčak-Mandelbrot empirical law[9] for the distribution of islands on the earth's surface states that the number of islands with area greater than some size A obeys $N(\text{area} > A) \propto A^{-B}$. Mandelbrot[9] explains this law by showing that, for a scaling system of islands where the combined coastlines are a fractal of dimension D, the number of islands with characteristic length $\lambda > L$ obeys $N(\lambda > L) \propto L^{-D}$. For simple individual islands with area $\propto \lambda^2$ we have $N(\text{area} > A) \propto A^{-D/2}$ for the distribution. In cases (such as percolation) where each island or cluster is itself a scaling shape, the dimension of an individual cluster boundary satisfies $D_C < D$. Consequently,[9] area $\propto \lambda^{D_C}$ and $N(\text{area} > A) \propto A^{-D/D_C}$. Since $N(\text{area} > A)$ is the integral of n_A above, scaling theory with $n_A \propto A^{-\tau}$ corresponds to $N(\text{area} > A) \propto A^{1-\tau}$ and $D/D_C = \tau - 1 \approx 1.05$.

Figure 2(b) shows $N(\text{area} > A)$ vs A for the same films as Fig. 2(a). The direct display of $N(\text{area} > A)$ eliminates the problem of choosing appropriate bin sizes for a histogram of $n_A(p)$. For p well below p_c, $N(\text{area} > A)$ decays rapidly for A beyond some characteristic size ξ. For p well above p_c, $N(\text{area} > A)$ becomes independent of A at large A. Near p_c, however, $N(\text{area} > A)$ is consistent with the expected $A^{-1.05}$ dependence for a large range of A.

Second-order phase transitions have power-law (rather than exponential) correlation functions at the critical point.[6] The probability, $g(R)$, that two points separated by a distance R are in the same cluster takes the form $g(R) \propto R^{-\eta}$ at p_c. Figure 3(a) shows the measured $g(R)$ for the Au films at different p. For $p < p_c$, $g(R)$ decays rapidly at large R while for $p > p_c$, $g(R)$ approaches a constant. At $p = 0.707$, below p_c, $g(R)$ shows a large power-law section with $\eta = 0.44 \pm 0.07$ but decreases more rapidly for $R > 500$ nm. At $p = 0.752$, on the other hand, just above p_c, $g(R)$ remains very close to a power-law form with $\eta = 0.17 \pm 0.02$ with a flattening just discernible at the largest R. The measured $g(R)$ is thus consistent with an accepted[1] $\eta \approx 0.2$ at p_c.

The universal exponent η is related to the cluster density profile, to the scaling of the largest cluster at p_c, and, consequently, to D_C. In particular,[1,3,5,9] $D_C = 1 + (d-\eta)/2 = d/(1+1/\delta) = d - \beta/\nu \approx 1.9$ for $d=2$. Figure 3(b) shows a direct estimate[9] of D_C through the variation in cluster shape with the minimum resolved length λ in the image. If the entire image of size $L \times L$ is divided into $(L/\lambda)^2$ squares of side λ, a D_C-dimensional object will intersect of order $(L/\lambda)^{D_C}$ squares. Thus, the fraction of squares intersected by the boundary, $f_s(\lambda)$, will vary as λ^{2-D_C}. For $p < p_c$, Fig. 3(b) shows that $f_s(\lambda) \to \lambda^2$ at large λ and all finite boundaries look pointlike ($D_C \to 0$) at large scales.

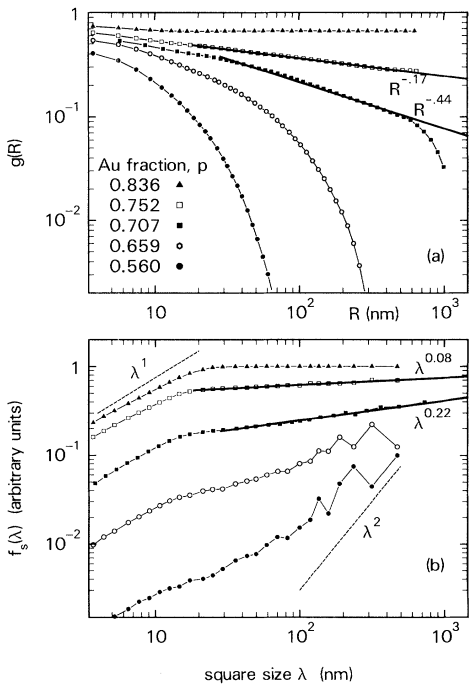

FIG. 3. (a) The probability $g(R)$ that two points separated by a distance R are in the same cluster. (b) The fraction of squares of size λ crossed by the boundary of the largest cluster $f_s(\lambda)$ as a function of λ. In both cases solid lines show power-law fits near p_c.

At large p and λ, $f_s(\lambda) \to \lambda^0$. Near p_c, however $f_s(\lambda)$ does scale as λ^{2-D_C} with $D_C \approx 1.78$ at $p = 0.707$ below p_c and $D_C \approx 1.92$ at $p = 0.752$ just above p_c. At small scales the correlated behavior with simple $D_C \approx 1$ boundaries is again visible as $f_s(\lambda) \propto \lambda^1$. Near p_c this measured D_C agrees with the η in Fig. 3(a) and the scaling relation $2-D_C = \eta/2$ and demonstrates experimentally the equivalence of the fractal analysis to the scaling exponents.

In conclusion, we have demonstrated that computer analysis of digitized micrographs can yield the high-quality statistics previously available only in simulations. We have used this technique to show that the large scale properties of actual Au films near the percolation threshold are consistent with random percolation. Local Au-Au and Au-substrate correlations, however, set a lower cutoff to the scaling behavior and raise p_c.[13] Finally, we have presented our measurements in terms of both standard percolation theory[1] and fractal geometry[9] and have demonstrated that the equivalence between the analytic[1] and geometric[9] scaling interpretations extends to actual metal films.

We are grateful to C. R. Guarnieri for expert sample preparation and to B. B. Mandelbrot, S. Kirkpatrick, Y. Imry, and Y. Gefen for illuminating discussions and helpful suggestions.

[1]See the excellent review by D. Stauffer, Phys. Rep. 54, 1 (1979), and references therein.

[2]S. Kirkpatrick, in *Electrical Transport and Optical Properties of Inhomogeneous Media—1977*, edited by J. C. Garland and D. B. Tanner, AIP Conference Proceedings No. 40 (American Institute of Physics, New York, 1978), p. 99, and in *Inhomogeneous Superconductors—1979*, edited by T. L. Francavilla, D. U. Gubser, J. R. Leibowitz, and S. A. Wolf, AIP Conference Proceedings No. 58 (American Institute of Physics, New York, 1979), p. 79.

[3]H. E. Stanley, J. Phys. A 10, L211 (1977).

[4]P. L. Leath, Phys. Rev. B 14, 5046 (1976).

[5]R. J. Harrison, G. H. Bishop, and G. D. Quinn, J. Stat. Phys. 19, 53 (1978).

[6]L. P. Kadanoff *et al.*, Rev. Mod. Phys. 39, 395 (1967).

[7]R. B. Laibowitz, E. I. Alessandrini, and G. Deutscher, Phys. Rev. B 25, 2965 (1982).

[8]See, for example, B. A. Abeles, H. L. Pinsh, and J. I. Gittleman, Phys. Rev. Lett. 35, 247 (1976); or C. J. Lobb, M. Tinkham, and W. J. Skocpol, Solid State Commun. 27, 1253 (1978).

[9]For a general discussion of fractals, see B. B. Mandelbrot, *The Fractal Geometry of Nature* (Freeman, San Francisco, 1982). Chapter 13 deals specifically with percolation.

[10]Y. Gefen, A. Aharony, B. B. Mandelbrot, and S. Kirkpatrick, Phys. Rev. Lett. 47, 1771 (1981).

[11]H. Kunz and B. Souillard, J. Stat. Phys. 19, 77 (1978); A. Coniglio and L. Russo, J. Phys. A 12, 545 (1979).

[12]S. Lovejoy, Science 216, 185 (1982).

[13]Although unnecessary for the measurements presented here, an accurate determination of p_c would require many more lower-magnification micrographs and would allow measurement of exponents such as ν and β that describe scaling away from p_c.

Percolation Characteristics in Discontinuous Thin Films of Pb

Aharon Kapitulnik and Guy Deutscher

Department of Physics and Astronomy, Tel Aviv University, 69978 Tel Aviv, Israel

(Received 6 August 1982)

The geometrical features of discontinuous Pb films are analyzed in terms of the scaling theory of percolation. Above the percolation threshold it is shown that the infinite cluster as well as the backbone has an anomalous mass distribution up to a length of the order of the percolation correlation length (ξ_p), corresponding to that of self-similar objects. Above ξ_p, the mass distribution is homogeneous. Below the percolation threshold, the cluster statistics agrees with scaling theory.

PACS numbers: 73.90.+f

The physical properties of thin mixture films have been investigated extensively in recent years, usually with metal and insulator coevaporated or cosputtered to form a metal-insulator mixture film.[1] A considerable amount of work has been done on the transport properties of such materials, most of the results reported being consistent with the predictions based on percola-

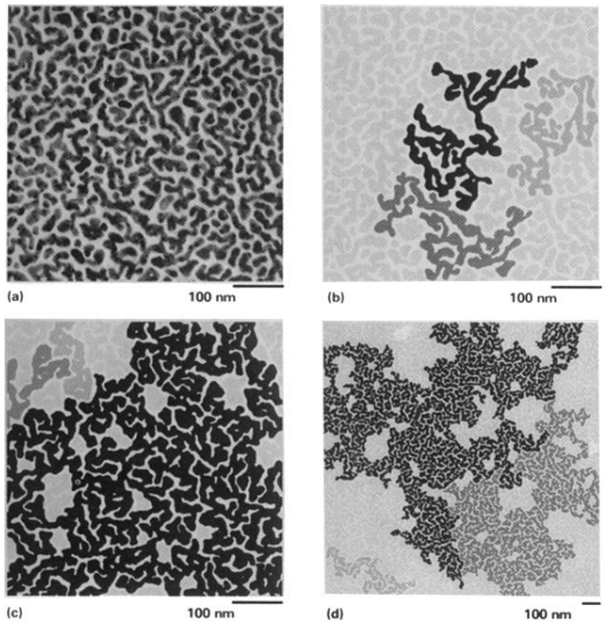

FIG. 1. (a) Halftone representation of a digitized Au cluster transmission electron micrograph. (b) Connectivity analysis of (a) with $p = 0.64$ with the largest clusters shown darkest. (c) Au clusters with $p = 0.75$. (d) Au clusters with $p = 0.71$ at a factor of 3 lower magnification.